Use of Atomistic Phonon Dispersion and Boltzmann Transport Formalism to Study the Thermal Conductivity of Narrow Si Nanowires

Hossein Karamitaheri[1,2], Neophytos Neophytou[1], and Hans Kosina[1]

[1] Institute for Microelectronics, TU Wien, Gußhausstraße 27-29/E360, A-1040 Wien, Austria

[2] School of Electrical Engineering, Sharif University of Technology, Tehran 11365-9363, Iran

E-mail: {karami | neophytou | kosina}@iue.tuwien.ac.at

Abstract

We study the thermal properties of ultra-narrow silicon nanowires with diameters from 3 to 12 nm. We use the modified valence-force-field method for the computation of the phononic dispersion and the Boltzmann transport equation for the phonon transport calculation. The phonon dispersion in ultra-narrow 1D structures differs from the bulk dispersion and the dispersion of thicker nanowires, which leads to different thermal properties. We show that as the diameter of the nanowire is decreased, the density of the long-wavelength phonons per cross section area increases, which increases their relative importance in carrying heat compared to the rest of the phonon spectrum. This effect, together with the fact that low-frequency, low-wavevector phonons are affected less by scattering and have longer mean-free-paths compared to phonons in the rest of the spectrum, leads to a counter-intuitive increase in the thermal conductivity as the diameter is reduced to the sub-ten nanometer range. This behavior is retained also in the presence of moderate boundary scattering.

Index terms: silicon nanowires, thermal conductivity, modified valence force field method, Boltzmann transport equation, low-dimensional effects.

I. Introduction

The thermal conductivity of bulk Si has a relatively high value of κ~140W/mK, and is dominated by phonon transport. In low-dimensional Si nanowires (NWs), on the other hand, significantly lower thermal conductivity values have been achieved, attributed to strong boundary scattering effects [1, 2, 3]. Numerous studies can be found in the literature regarding the thermal conductivity of Si NWs [4, 5, 6, 7, 8]. The effects of different scattering mechanisms, i.e. surface roughness scattering, mass doping, phonon-phonon scattering, and phonon-electron scattering have been investigated by several authors [9, 10, 11, 12]. The phonon dispersion in low-dimensional materials, however, is different from the bulk dispersion. For ultra-narrow NWs, i.e. below 10nm in diameter, the effect of confinement can further change the phonon spectrum significantly, and thus the thermal properties.

To date the effects of nanostructuring on the structure of phonon modes in low-dimensional channels and their influence on thermal conductivity are still not well understood. It is common practice in simulation studies to use either continuum approaches or the Si bulk dispersion (even in a confined geometry) [9, 7, 13, 14, 15]. Other studies use purely diffusive boundary scattering (specularity parameter p=0) [16, 17, 14], or the same scattering probability for all phonon states with different wavelength (p=constant) [9, 18], which is effective in explaining experimental measurements for confinement length scales down to several tens of nanometers. However, the phonon mode dispersion and density of states undergo strong modifications in nanostructures and the atomistic description of the phonon dispersion and the wave nature of phonons acquires significant importance.

In this work, we employ the modified valence force field method (MVFF) [19,20] along with the ballistic Landauer formalism and the diffusive Boltzmann transport equation for phonons to address the effects of structural confinement of the phonons on the thermal properties of low-dimensional Si NWs of diameters from 12 nm down to 3nm. We show that the long-wavelength phonons turn out to be much more significant in 1D systems than they are in bulk material. Their density, as well as their

significance compared to the rest of the spectrum increases as the diameter is reduced, which results in more than ~60% of the heat being carried by these long-wavelength, low energy phonons, which in turn undergo relatively weak scattering [21]. This results in a counter-intuitive increase in thermal conductivity with diameter reduction, which is retained even in the presence of moderate boundary scattering. We finally show that due to the specular scattering nature of the long-wavelength phonons on the boundaries under weak roughness amplitudes, a large portion of the heat is carried by phonons with mean-free-paths significantly larger than the NW diameter.

II. Approach

For the calculation of the phononic bandstructure we employ the modified valence force field method [19], which is an extension of the Keating model [22]. In this method the inter-atomic potential is modeled by the following bond deformations: bond-stretching, bond-bending, cross-bond-stretching, cross-bond-bending-stretching, and coplanar-bond-bending interactions [19]. The model accurately captures the bulk Si phonon spectrum as well as the effects of confinement in NWs [20]. As an empirical atomistic model, its parameters are calibrated to the bulk dispersion, in this case over the entire Brillouin zone. This is common practice for electronic structure methods as well (e.g. the use of tight-binding, pseudo-potential, and k.p methods for the electronic properties of nanostructures). Transferability of the model parameters for nanostructures is then assumed. Of course the only true verification is comparison to experimental measurements, which at this point are sparse for NWs, especially of such ultra-narrow diameters. Typical phonon modes for NWs are shown in Fig. 1. Figures 1a, 1b and 1c show the lower energy part of the dispersions of the <111> oriented NWs of diameters D=12nm, 6nm, and 3nm, respectively. We note that without loss in generality we use the <111> transport orientation in this manuscript unless otherwise specified. The phonon spectrum of the thicker NWs consists of many more modes than thinner NWs do. The lowest four acoustic branches, however, other than some changes in their shape, remain

the same as the diameter is reduced. The energy region in which only these four bands contribute is shown by the curly brackets in each NW case. Because the number of these bands remains the same, although the diameter is reduced, their density per unit of cross section area increases. As we show below, this has strong consequences in the thermal conductivity of the NWs.

After calculating the phonon dispersion, the thermal conductivity is obtained assuming the phonon relaxation time approximation in the phononic Boltzmann transport equation as [23, 13]:

$$\kappa_l = k_{\mathrm{B}} \sum_{i,q} \tau_i(q) v_{\mathrm{g},i}(q)^2 \left[\frac{\hbar \omega_i(q)}{k_{\mathrm{B}} T} \right]^2 \frac{e^{\hbar \omega_i(q)/k_{\mathrm{B}} T}}{\left(e^{\hbar \omega_i(q)/k_{\mathrm{B}} T} - 1 \right)^2} \tag{1}$$

where k_{B} is the Boltzmann constant, $v_{\mathrm{g},i}$ is the group velocity of a phonon of wavevector q in subband i, given by $v_{\mathrm{g},i}(q) = \partial \omega_i(q) / \partial q$, and $\tau_i(q)$ is the scattering time. For the calculation of the relaxation times, we follow the bulk formalisms for Umklapp scattering as [24, 25, 9]:

$$\frac{1}{\tau_U} = B \omega_i(q)^2 T \exp(-\frac{C}{T}) \tag{2}$$

where $B = 2.8 \times 10^{-19}$s/K and $C = 140$K [26]. This is the simplest model available for Si, calibrated to the bulk thermal conductivity over a large temperature range [26]. Although the model assumes 3D phonons, it is commonly employed in the calculation of the thermal conductivity in nanostructures as well [9, 18, 26]. The reason why such a model derived for 3D channels provides sufficient accuracy for nanostructures, is that even for 1D channels the atomic vibrations are still in 3D and not constrained in one particular direction [27]. Modifications and extensions of this transport model are described in the literature to improve its validity for nanostructures, still under the assumption of 3D phonons [28, 29]. One of these modifications proposed by Mingo *et* al. is employed here and described further on [27]. Another reason is that the dominant scattering mechanism in low-dimensional channels is boundary scattering rather than phonon-phonon scattering, and, therefore, the accuracy of the phonon-phonon scattering model will have only little influence on the accuracy of the overall thermal conductivity of nanostructures [9].

For boundary scattering we use the Casimir formula:

$$\frac{1}{\tau_{B,i}(q)} = \frac{1-p(q)}{1+p(q)} \frac{v_{g,i}(q)}{D} \tag{3}$$

where D is nanowire's diameter and $p(q)$ is q-dependent specularity parameter given by [21, 23, 13]:

$$p(q) = \exp(-4q^2\Delta_{rms}^2) \tag{4}$$

We vary the root-mean-square of the roughness amplitude as Δ_{rms} from 0.1 nm to 1.2 nm. In this model the scattering rate depends on the confinement size D (inversely) and the specularity parameter p. It is again based on the assumption of 3D phonon scattering on boundaries. Although commonly employed in low-dimensional nanostructures [9, 28, 13], strictly speaking its validity can be questioned for ultra-narrow 1D NWs since one cannot define a transverse phonon velocity in a purely 1D system. The model implies that the phonons are isotropic, i.e. they will travel towards the surface with the same velocity as along the wire axis. Using atomistic calculations, however, Carette *et* al., in Ref. [30] have recently shown that even in the case of ultra-thin NWs of diameter ~2nm and with roughness amplitude as large as 20%, the phonon mean-free-path and the thermal conductivity are very close to what the Casimir limit predicts [30] (for p=0). The Casimir model breaks down at much stronger roughness strength where strong boundary effects appear. Here, the specularity parameter is higher for low frequency/long wavelength phonons since long waves are only little affected by the short range roughness. As the scattering rate is inversely proportional to the specularity parameter (Eq. 3), the mean-free-path of low frequency phonons is longer than that of high frequency phonons. This feature of the Casimir model is also in good agreement with atomistic calculations [30, 31]. The Casimir model (Eq. 3), therefore, captures basic features of boundary-scattering down to ultra-narrow NWs, although the boundary scattering is phenomenologically different in 3D and 1D channels. In this work, however, we consider quasi-1D NWs down to D=3nm in diameter, and limit the roughness amplitude to 10% of the NW's diameter.

III. Results and Discussion

Because the density of the low-frequency, long-wavelength phonon modes increases with diameter reduction as mentioned above, their importance in the NWs heat carrying capabilities increases. A simple, but effective way to demonstrate this, is by plotting the differential (or frequency spectrum) of the ballistic thermal conductance versus energy for NWs of different diameters, as shown in Fig. 2a. The differential of the ballistic thermal conductance (normalized by the NW area *A*) at a specific energy is calculated as [32, 33 , 34]:

$$\frac{dK_l(\omega)}{Ad\omega} = \frac{\pi {k_B}^2 T}{6A} \sum_i \int v_{g,i}(q) W_{ph.}(\hbar\omega) \delta\left(\omega - \omega_i(q)\right) dq \qquad (5)$$

where $W_{ph.}(\hbar\omega)$ is the phonon window function that determines the conductance, defined as [26, 35]:

$$W_{ph.}(\hbar\omega) = \frac{3}{\pi^2 k_B T} \left[\frac{\hbar\omega}{k_B T}\right]^2 \frac{e^{\hbar\omega/k_B T}}{\left(e^{\hbar\omega/k_B T} - 1\right)^2} \qquad (6)$$

Under ballistic conditions, the entire energy spectrum contributes to the thermal conductance. This is contrary to what would be expected from diffusive transport, in which case the low-frequency modes dominate the thermal conductivity. The reason is that the phonon window function shown in Fig. 2b (blue line) is a wide and flat function at room temperature, covering most of the energy spectrum [35]. For the thicker NWs in Fig. 2a, i.e. for *D*=12nm (green-triangle line), the high frequency phonons contribute the most because the number of modes is larger at higher frequencies. As the diameter is reduced down to *D*=3nm, however, although the high frequency phonons still contribute the most, the contribution of the low-frequency modes increases. If smaller diameters are considered (*D*=1nm and *D*=2nm), the contribution of the low frequency modes is even stronger (note that these two curves are shown in dashed lines as indication to what could happen, although for such low diameters we might be already reaching the limits of the transferability of the MVFF model parameters in calculating the NW phonon dispersion). The increasing contribution of the low frequency phonons is attributed to the fact that the density of these modes increases. Indeed, ultra-narrow NWs have a finite phonon density-

of-states (DOS) at low frequencies, in contrast to bulk, in which case the phonon density-of-states tends to zero. A consequence of this increase in the phonon DOS at low frequencies as shown in Fig. 2a, is that their contribution to the ballistic thermal conductance increases as the NW diameter is reduced. In the next sections of the paper, we examine the consequences of this effect once scattering is included, and whether this increase could be retained.

Due to the finite DOS that is introduced at low-frequencies with decreasing diameter, the use of the bulk model for Umklapp scattering as in Eq. 2, causes divergence in the thermal conductivity. To avoid this divergence, either the bulk dispersion or the constant specularity parameters for phonon-boundary roughness are commonly used in the literature. This partially neglects the wave nature of phonons. However, as proposed by Mingo *et* al., an additional scattering mechanism for a second order 3-phonon process (as an order of magnitude approximation) can be introduced as [27]:

$$\frac{1}{\tau_{U2}} = A_0 T^2, \tag{7}$$

in order to remove this singularity for the low frequency phonons. Here A_0 is used as a fitting parameter to match the extracted thermal conductivity to more sophisticated models. The use of such frequency-independent contribution in the calculation of the scattering rate is actually similar to imposing a lower frequency cut-off in the integration over the phonon spectrum (or imposing a finite channel length as in the direct methods), methods which also remove the singularity at zero frequency.

Due to this simplified treatment of the second order 3-phonon processes, quantitative values for the thermal conductivity can only be obtained by fitting to more sophisticated calculations as reliable experimental data are unavailable. Using a value of $A_0 = 15000 / \mathrm{sK}^2$, we benchmark our results with more sophisticated calculations for the thermal conductivity by Luisier [36] who used the direct NEGF method and Donadio *et* al. who used molecular dynamics [37]. Figure 3 shows this comparison between our calculations (lines) for the thermal conductivity versus temperature and those of Ref. [36] (symbols) for the *D*=3nm diameter NWs in the <100>, <110>, and the <111> transport

orientations, as well as the result of Ref. [37] for the <100> NW. The comparison is very close for all three NW orientations, especially for temperatures above 200K. The deviation is larger at lower temperatures, because our choice of A_0 was from a calibration at room temperature. A different choice of A_0 would provide a better match at lower temperatures. We should note, however, that a direct comparison with Luisier's data for low temperature, where the low-wavevector modes determine the conductivity is not possible. The calculations of Luisier employ the direct method, in which the thermal conductivity depends on the length of the channel considered (up to 75 nm in that work). The longer the channel length, the more low frequency modes participate, and the higher is the thermal conductivity. The thermal conductivity finally saturates at the diffusive value as the channel length goes to infinity. This has recently been experimentally and theoretically reported in the case of graphene nanoribbons even at room temperature [38, 31]. Therefore, the higher thermal conductivity in our calculations compared to the work of Luisier at low temperatures can be partially attributed to the finite channel length used by Luisier.

The increasing importance of the long-wavelength phonons for ultra-narrow NWs is demonstrated in Fig. 4a, which shows the differential contribution to the Umklapp-limited thermal conductivity of phonons with different frequencies. We show results for three different NW diameters, D=12nm, 6nm, and 3nm. It is evident that the low frequency phonons contribute the most to the thermal conductivity. This is particularly pronounced in the case of the narrower NWs. The thermal conductivity of phonons with energies below ~10-15 meV is almost two orders of magnitude higher than that of phonons of higher energies (note the logarithmic scale in Fig. 4a). Figure 4b shows the cumulative thermal conductivity of these NWs versus energy. Two very interesting observations can be made here: i) Most of the contribution to the total thermal conductivity is attributed to phonons of energies below 10meV, especially in the case of NWs with diameters D=3nm and 6nm. ii) The most interesting observation is that the Umklapp-limited thermal conductivity is larger for the thinner NWs. The thermal conductivity of the D=12nm NW is reduced from the bulk value (κ_{bulk}~140 W/mK) down to ~15 W/mK. This is attributed to the reduction of the phonon group velocity and

changes in the phonon spectrum due to confinement [29, 39]. As the diameter is decreased even further, however, the increasing contribution of the long-wavelength phonons causes the thermal conductivity to increase again. The reasons for this are: i) The density of these modes increases compared to the rest of the spectrum as described in the ballistic results of Fig. 2a. ii) The low-frequency, low-wavevector modes undergo weaker scattering, compared to the high frequency modes. The window function in the case of phonon-phonon limited transport in Fig. 2b (red line) is now multiplied by the phonon-phonon scattering lifetime as $\tau_{ph.-ph.}W_{ph.}$ (see Eq. 1), which makes it a much narrower energy function, allowing mostly the low frequency modes to participate in transport. Therefore, as the density of these important modes increases with diameter reduction, the thermal conductivity increases. We note that this counter-intuitive effect is also observed in more sophisticated molecular dynamics calculations by Donadio *et* al. [37]. The fact that the narrowing of the phonon window function is a general feature of phonon transport, explains why our simplified Umklapp model based on 3D phonons also captures this effect (at least qualitatively) which originates from the increase in low-wavevector, low-frequency mode density. The reason why $\tau_{ph.-ph.}W_{ph.}$ is narrower thatn $W_{ph.}$ is because low-frequency, low-wavevector phonons have larger mean-free-paths and relaxation times. Note that the function $\tau_{ph.-ph.}W_{ph.}$ can even be narrower if one uses the exact solution of Boltzmann transport equation. In this case, the selection rules (to ensure energy and momentum conservation) are valid only at some points of the dispersion, rather than on lines or surfaces in 2D and 3D respectively [27]. This could indicate that in low dimensional materials phonon-phonon scattering is weaker. Our calculations show that for the D=1nm NW the thermal conductivity can increase back to the bulk value (not shown), in very good agreement with molecular dynamics calculations [37], although the accuracy of our model could be questionable at such low diameters. We should also note that this narrowing of the $\tau_{ph.-ph.}W_{ph.}$ function is not sensitive to the value of A_0 we use to calibrate our data, even if A_0 increases or decreases by an order of magnitude.

This counter-intuitive increase in the thermal conductivity with diameter reduction is also retained in the presence of phonon-boundary scattering on top of

Umklapp scattering. Figure 5a, as in the case of Fig. 4a, shows the differential contribution to the thermal conductivity of phonons with different energies, again for the NWs with diameters D=12nm (green), 6nm (red), and 3nm (blue). Compared to Fig. 4a, the inclusion of boundary scattering in Fig. 5a, reduces the differential values of the thermal conductivity, but also redistributes the thermal conductivity to a much narrower energy region below 5meV (see the peak of $d\kappa_l/d\omega$ around E=0eV in Fig. 5a). These phonons are affected by boundary scattering the least. The reason is that the specularity parameter $p(q)$ in Eq. 4 peaks at q=0 indicating specular scattering, and drops sharply for higher energies. As shown in Fig. 5b (right side), although the overall thermal conductivity drops to significantly lower values due to boundary scattering compared to Fig. 4b, the higher thermal conductivity of the D=3nm compared to the D=12nm NW, is still retained for small roughness amplitude (Δ_{rms}=0.1nm). One would have expected that the narrower the diameter is, the more effectively boundary scattering reduces the thermal conductivity. This would have been true if the boundary scattering rate in Eq. 3 was only proportional to 1/D. The term $(1-p)/(1+p)$ in Eq. 3, however, approaches zero as p approaches unity for low-q phonons. This reduces the scattering rate for these phonons. Since their importance increases with diameter reduction, the overall scattering in the narrower NWs decreases and the thermal conductivity increases. As the roughness amplitude increases, however, the increase in the Umklapp-limited thermal conductivity of the narrower NWs is lost as the boundary scattering eventually becomes stronger with decreasing NW diameter (see second and third set of lines in Fig. 5b for Δ_{rms}=0.3nm and Δ_{rms}=0.6nm).

The change in thermal conductivity with reducing the dimensionality of the system is an important design parameter for thermal management and thermoelectric applications. In the case of thermal management in nanoscale electronic devices, a large thermal conductivity removes the heat from the device and is actually desired. In the case of thermoelectric devices, on the other hand, thermal conductivity needs to be reduced in order to retain the temperature gradient between the hot and cold sides of the device and reduce losses. For properly designing such channels, the relevant quantity that needs to be taken into consideration is the mean-free-path (MFP) of the phonons that contribute to

thermal conductivity. In the case of thermoelectric devices, for example, the design strategy to reduce thermal conductivity is to introduce scatterers of the order of the dominant MFPs [40]. The MFP of each phonon state in the case of 1D NWs is given by the product of the phonon group velocity and relaxation time as $\lambda_i(q) = v_{g,i}(q)\tau_i(q)$. In Fig. 6a we extract the cumulative thermal conductivity versus the MFP of the phonons for the *D*=12nm NW. We show cases for Umklapp-limited scattering (black line) and Umklapp plus boundary limited scattering with different Δ_{rms} values for the scattering strength (Δ_{rms} =0.1nm, 0.3nm, and 1.2nm – up to 10% of the NW diameter). The red arrow indicates the 12nm MFP, same as the diameter of the NW. In the case of Umklapp scattering the MFP of the phonons that contribute to thermal conductivity is distributed more or less uniformly from 1nm to 6μm (similar to what is reported for bulk Si [41, 26]). The large MFPs contribute strongly to heat as observed in the inset of Fig. 6a. Here we show a part of the phonon spectrum of this NW. The colormap shows the contribution to the thermal conductivity of each of the phonon states in the case of Umklapp-limited scattering. In red we show the large contribution to κ_l, and in blue the small contribution. The larger contribution comes from the longer MFPs of the LA branch. With the introduction of boundary scattering, on the other hand, the overall thermal conductivity is strongly reduced, but the distribution of heat within the different phonon MFPs changes as well. A slightly larger part of the heat compared to the case of Umklapp-limited scattering is now carried by phonons of MFPs below 12nm, whereas long-wavelength phonons now carry less heat (right side of Fig. 6a). For small roughness amplitude, although reduced, this amount is still significant, indicating that MFPs larger than the NW diameter still contribute significantly to the thermal conductivity ~~due to their almost specular *p(q)*~~. For relatively strong roughness (green line, Δ_{rms}=1.2nm, 10% of the diameter), on the other hand, the MFPs are limited to values below the NW diameter, which indicates that the scattering approaches the Casimir limit (black-dashed line), i.e. the phonon-boundary scattering MFP is limited by the diameter of the NW. The green line in Fig. 6a, therefore, saturates after MFPs of ~12nm. An interesting observation can be made in Fig. 6b, which shows the same quantity for the narrower NW with *D*=3nm. The Casimir limit is reached for relatively larger percentage of roughness amplitudes (above Δ_{rms}=0.6nm, i.e. 20% of the NW's diameter, although this could be pushing the

limits of our model). This is indicated by the fact that the green line in Fig. 6b still slightly increases for MFPs above ~3nm. It is because the scattering of the low-wavevector states is more specular, and since their density in the phonon spectrum increases, the overall phonon MFP increases. It also explains why phonons with MFPs larger than the NW's diameter contribute significantly to the thermal conductivity at least for weak roughness. Note that more sophisticated calculations at an atomistic level indicate that indeed the Casimir limit can describe the influence of boundary scattering in NWs of diameters even down to 2nm and roughness amplitude even up to 20% [30]. This is quite interesting since the Casimir formula is a simplified treatment actually based on 3D phonons scattering on the boundaries rather than on 1D phonons.

IV. Conclusions

In this work we study the thermal properties of ultra-narrow silicon nanowires using the atomistic modified valence force field method for the computation of the phonon bandstructure and the ballistic Landauer approach as well as lifetime approximation solution of the phononic Boltzmann transport equation for the calculations of ballistic and diffusive thermal conductivities, respectively. We address the effects of structural confinement on the phonon dispersion and its consequences on the thermal conductivity. We show that the thermal conductivity is significantly reduced from the bulk values as the NW diameter is reduced down to D=12nm due to phonon bandstructure changes ~~reduction~~. For ultra-narrow NWs of diameters down to ~~below~~ 3nm, however, the thermal conductivity increases again due to the increasing density of the long-wavelength phonons, which undergo weaker scattering. This behavior is also retained in the presence of moderate boundary scattering. Finally, we show that a significant amount of heat in NWs is transported by phonons of mean-free-paths longer than the nanowire's diameter, especially in the narrower nanowires. In this case, the Casimir limit is reached for relatively large roughness of the order of 20% of the diameter.

Acknowledgements

The work leading to these results has received funding from the European Community's Seventh Framework Programme under grant agreement no. FP7-263306.

References

[1] A. I. Boukai, Y. Bunimovich, J. Tahir-Kheli, J.-K. Yu, W. A. Goddard, and J. R. Heath, *Nature*, vol. 451, pp. 168-171, 2008.

[2] A. I. Hochbaum, R. Chen, R. D. Delgado, W. Liang, E. C. Garnett, M. Najarian, A. Majumdar, and P. Yang, *Nature*, vol. 451, pp. 163-168, 2008.

[3] J. Lim, K. Hippalgaonkar, S. C. Andrews, A. Majumdar, and P. Yang, *Nano Lett.*, 12, 2475–2482, 2012.

[4] I. Ponomareva, D. Srivastava, and M. Menon, *Nano Letters*, vol. 7, pp. 1155-1159, 2007.

[5] N. Yang, G. Zhang, and B. Li, *Nano Letters*, vol. 8, pp. 276-280, 2008.

[6] S.-C. Wang, X.-G. Liang, X.-H. Xu, and T. Ohara, *J. Appl. Phys.*, vol. 105, p. 014316, 2009.

[7] M. Liangraksa and I. K. Puri, *J. Appl. Phys.*, vol. 109, p. 113501, 2011.

[8] J. H. Oh, M. Shin, and M.-G. Jang, *J. Appl. Phys.*, vol. 111, p. 044304, 2012.

[9] N. Mingo, *Phys. Rev. B*, vol. 68, p. 113308, 2003.

[10] X. Lu and J. Chu, *J. Appl. Phys.*, vol. 100, p. 014305, 2006.

[11] M.-J. Huang, W.-Y. Chong, and T.-M. Chang, *J. Appl. Phys.*, vol. 99, p. 114318, 2006.

[12] P. Martin, Z. Aksamija, E. Pop, and U. Ravaiolo, *Phys. Rev. Lett.*, vol. 102, p. 125503, 2009.

[13] Z. Aksamija and I. Knezevic, *Phys. Rev. B*, 82, 045319, 2010.

[14] J. E. Turney, A. J. H. McGaughey, and C. H. Amon, *J. Appl. Phys*., 107, 024317, 2010.

[15] Z. Tian, K. Esfarjani, J. Shiomi, A. S. Henry, and G. Chen, *Appl. Phys. Lett.*, 99, 053122, 2011.

[16] W. Liu and M. Asheghi, *J. App. Phys.*, vol. 98, p. 123523, 2005.

[17] W. Liu and M. Asheghi, *J. Heat Transfer*, vol. 128, p. 75, 2006.

[18] N. Mingo, L. Yang, D. Li, and A. Majumdar, "Predicting the Thermal Conductivity of Si and Ge Nanowires", *Nano Lett.*, 3, 12, 1713-1716, 2003.

[19] Z. Sui and I. P. Herman, *Phys. Rev. B*, 48, 17938-17953, 1993.

[20] A. Paul, M. Luisier, and G. Klimeck, *J. Comput. Electron.*, 9, 160-172, 2010.

[21] J. M. Ziman, "*Electrons and Phonons: The Theory of Transport Phenomena in Solids"*, Clarendon, Oxford, 1962.

[22] P. N. Keating, *Phys. Rev.*, vol. 145, pp. 637– 645, 1966.

[23] G. P. Srivastava, *"The Physics of Phonons"*, Taylor & Francis Group, New York, 1990.

[24] M. G. Holland, *Phys. Rev.*, 132, 6, 2461-2471, 1963.

[25] M. Asen-Palmer, K. Bartkowski, E. Gmelin, M. Cardona, A. P. Zhernov, A. V. Inyushkin, A. Taldenkov, V. I. Ozhogin, K. M. Itoh, and E. E. Haller, *Phys. Rev. B* **56**, 9431, 1997.

[26] C. Jeong, S. Datta, and M. Lundstrom, *J. Appl. Phys.*, 111, 093708, 2012.

[27] N. Mingo, D. A. Broido, *Nano Lett.*, 5, 1221-1225, 2005.

[28] E. B. Ramayya, L. N. Maurer, A. H. Davoody, and I. Knezevic, *Phys. Rev. B*, 86, 115328, 2012.

[29] J. Zou and A. Balandin, *J. Appl. Phys.* 89, 2932, 2001.

[30] J. Carrete, L. J. Gallego, L. M. Varela, N. Mingo, *Phys. Rev. B*, 84, 075403, 2011.

[31] H. Karamitaheri, M. Pourfath, R. Faez, H. Kosina, *IEEE Transactions on Electron Devices*, 60, 2142, 2013.

[32] Z. Aksamija and I. Knezevic, *J. Comput. Electronic*, 9, 173, 2010.

[33] H. Karamitaheri, N. Neophytou, and H. Kosina, *J. Appl. Phys.*, 113, 204305, 2013.

[34] H. Karamitaheri, N. Neophytou, M. K. Taheri, R. Faez, and H. Kosina, *J. Electr. Materials*, 42, 2091, 2013.

[35] T. Markussen, A.-P. Jauho, and M. Brandbyge, Nano Lett., 8, 3771, 2008.

[36] M. Luisier, “Atomistic Modeling of Anharmonic Phonon-Phonon Scattering in Nanowires”, *Phys. Rev. B*, vol. 86, p. 245407, 2012.

[37] D. Donadio, and G. Galli, *Nano Lett.*, 10, 847-851, 2010.

[38] M.-H. Bae, Z. Li, Z. Aksamija, P. N Martin, F. Xiong, Z.-Y. Ong, I. Knezevic, and E. Pop, *Nature Communications*, 4, 1734, 2013.

[39] X. Lu, *J. Appl. Phys.*, 104, 054314, 2008.

[40] K. T. Regner, D. P. Sellan, Z. Su, C. H. Amon, A. J.H. McGaughey, and J. A. Malen, *Nature Comunications*, 4, 16040, 2013.

[41] M. Zebarjadi, K. Esfarjani, M. S. Dresselhaus, Z. F. Ren and G. Chen, *Energy Environ. Sci.*, 5, 5147, 2012.

Figure 1:

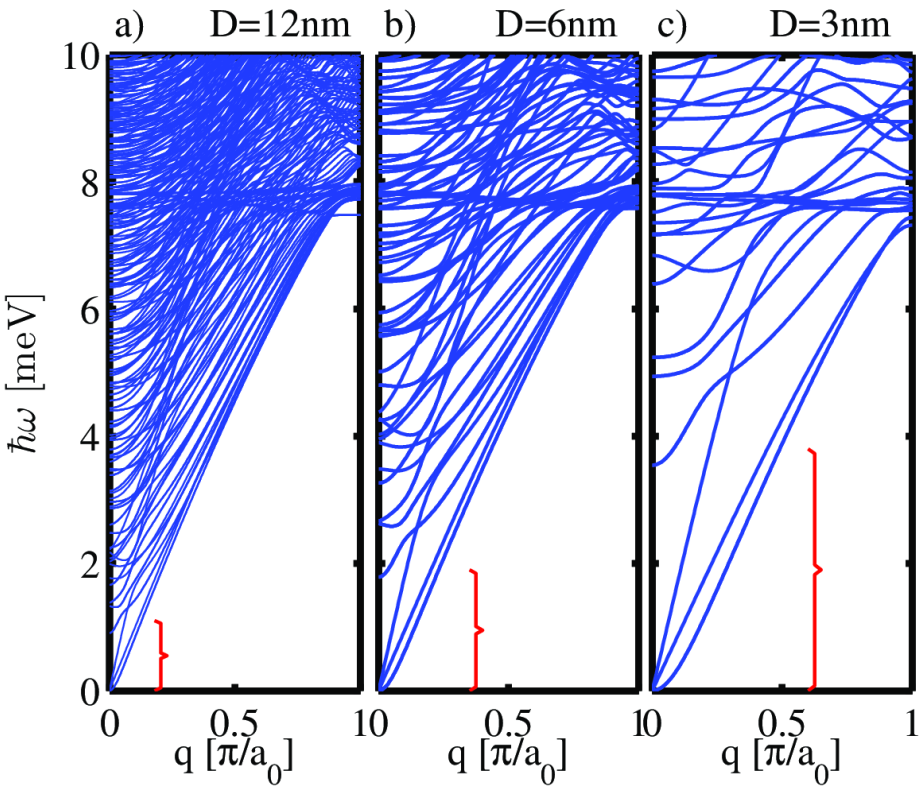

Figure 1 caption:

Phonon dispersions for (a) *D*=12nm, (b) *D*=6nm, and (c) *D*=3nm NWs in the <111> transport orientation. As the diameter is decreased, the number of phonon modes is also reduced. The lowest four acoustic modes at low frequencies, however, remain, as indicated by the curly brackets.

Figure 2:

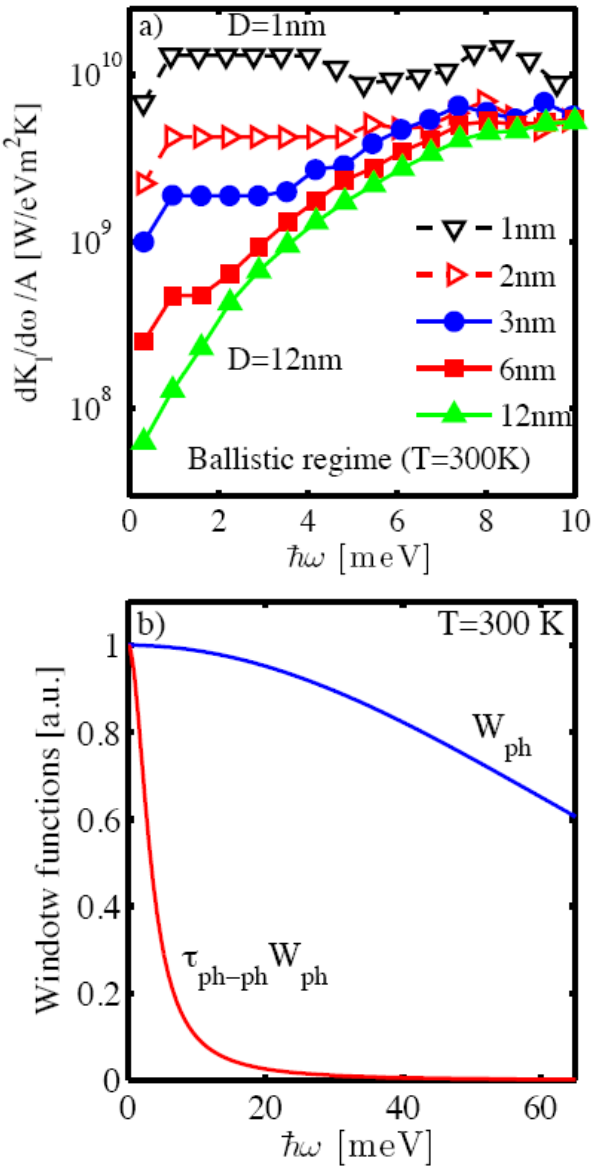

Figure 2 caption:

(a) The differential contribution to the ballistic thermal conductance of phonons of different energies. Nanowire diameters as they appear from top to bottom in the low energy region: $D=1\text{nm}$, $D=2\text{nm}$, $D=3\text{nm}$, $D=6\text{nm}$ and $D=12\text{nm}$. The contribution of the low frequency modes increases with reducing diameter. (b) The phonon window function that determines the thermal conductance in the cases of ballistic (blue) and Umklapp-limited scattering (red).

Figure 3:

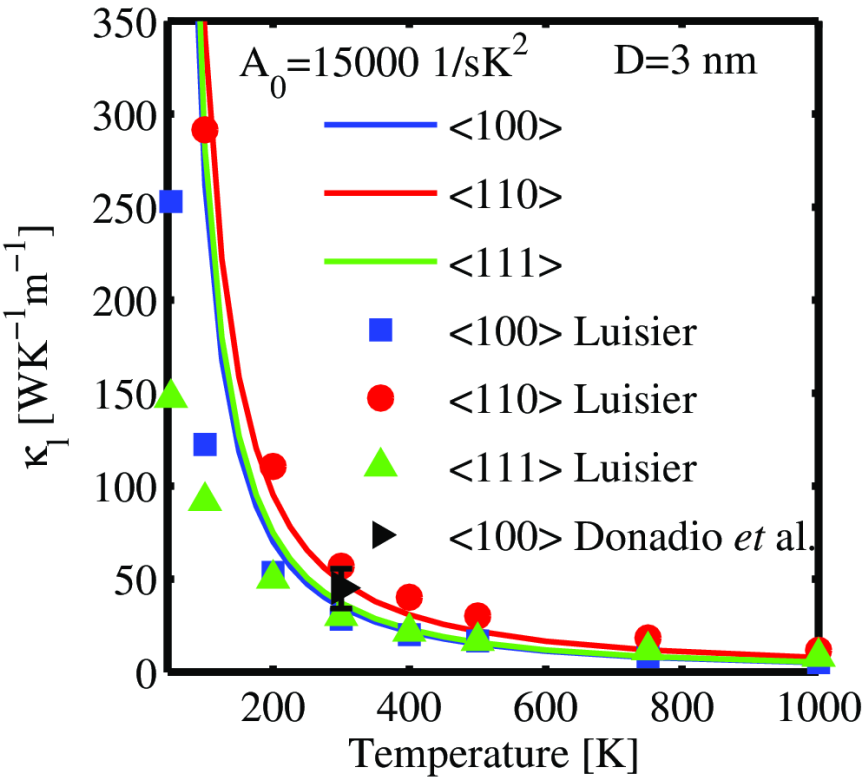

Figure 3 caption:

The Umklapp-limited thermal conductivity versus temperature for NWs with *D*=3nm in the <100> (blue line), <110> (red line), and <111> (green line) transport orientations. The dots are results from calculations by Luisier [36] for the same NWs. Triangle is the results by Donadio *et* al. [37].

Figure 4:

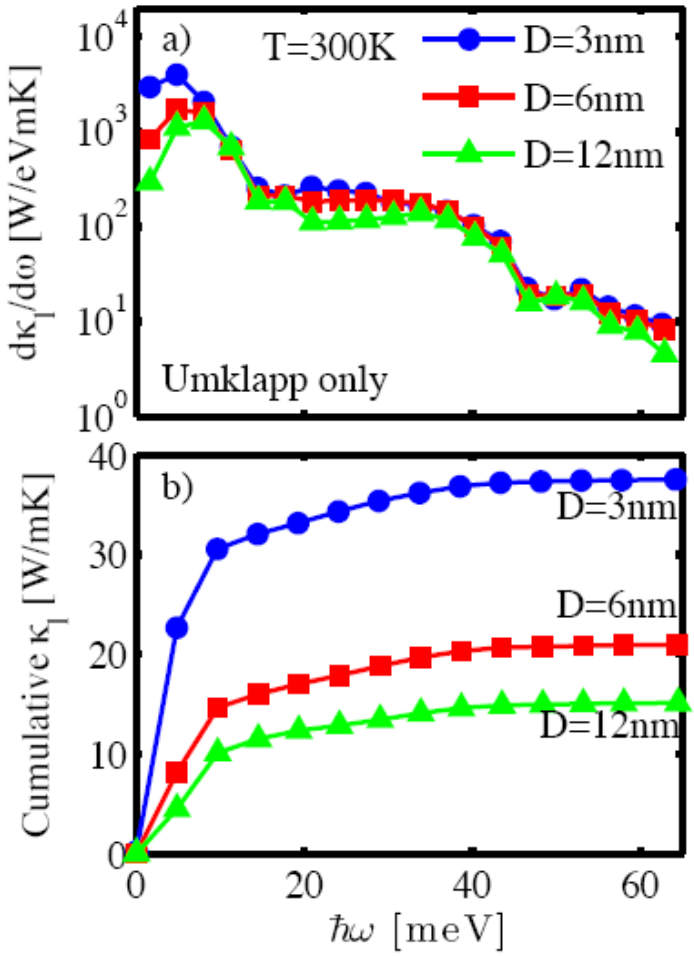

Figure 4 caption:

(a)The differential contribution to the Umklapp-limited thermal conductivity of phonons of different energies. Nanowire diameters as they appear from top to bottom in the low energy region: $D = 3\text{nm}$, $D = 6\text{nm}$ and $D = 12\text{nm}$. (b) The cumulative thermal conductivity versus phonon energy. Nanowire diameters *D*=3nm (blue-dotted), *D*=6nm (red-squared), and *D*=12nm (green-triangled) are shown. The thermal conductivity increases by decreasing diameter due to the increase in the contribution of low frequency phonons which undergo less scattering.

Figure 5:

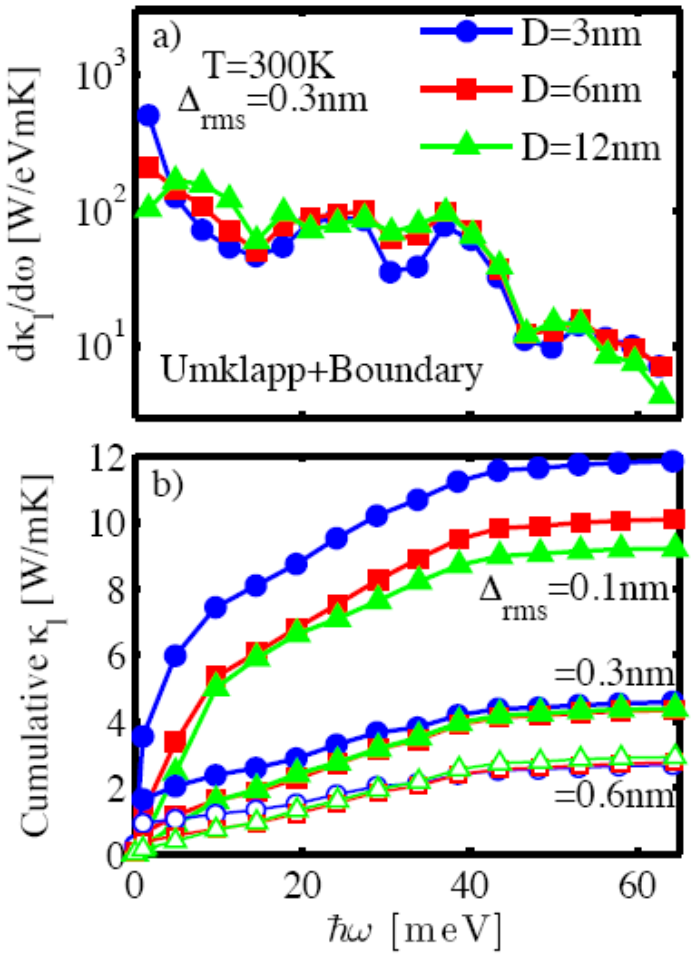

Figure 5 caption:

(a) The differential contribution to the Umklapp plus boundary scattering limited thermal conductivity of phonons of different energies. Nanowire diameters as they appear from top to bottom in the low energy region: $D = 3\text{nm}$, $D = 6\text{nm}$ and $D = 12\text{nm}$. (b) The cumulative thermal conductivity versus phonon energy. Nanowire diameters D=3nm (blue-dotted), D=6nm (red-squared), and D=12nm (green-triangled) are shown. Cases for boundary-scattering Δ_{rms} values of 0.1nm, 0.3nm and 0.6nm are shown.

Figure 6:

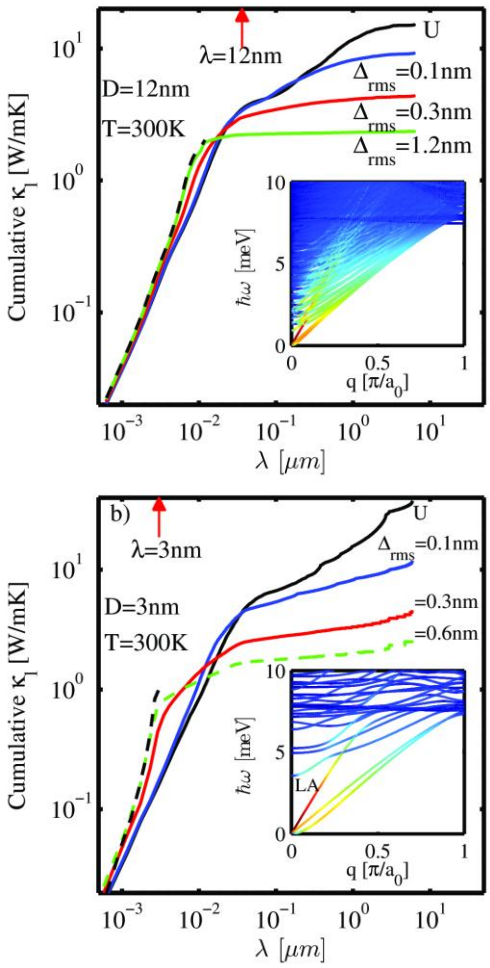

Figure 6 caption:

Cumulative thermal conductivity of the (a) *D*=12nm and (b) *D*=3nm <111> NW versus mean-free-path (MFP). Umklapp-limited thermal conductivity is shown by the black line. Umklapp plus boundary scattering thermal conductivity for Δ_{rms} values 0.1nm, 0.3 nm and 1.2 nm are shown by the blue, red and green lines, respectively in (a). In (b) Δ_{rms} values 0.1nm, 0.3 nm and 0.6 nm are shown (Δ_{rms} =0.6nm is dotted as an indication since at this value the limits of the model are reached). The MFP values of 12nm and 3nm, same as the diameter of the NWs are indicated on the x-axis. Fully diffusive boundary case (Casimir limit) is shown by black-dashed lines. Insets: Part of the NW's phonon dispersion, in which the colormap shows the contribution of each phonon state to the total thermal conductivity (red: largest contribution, blue: smallest contribution).